Spatio-Temporal Patterns Generated by *Salmonella typhimurium*

D. E. Woodward,*‡ R. Tyson,* M. R. Myerscough,§ J. D. Murray,* E. O. Budrene,¶ and H. C. Berg¶

*Department of Applied Mathematics FS-20, University of Washington, Seattle, Washington 98195 USA; ‡Department of Mathematics, Southern Methodist University, Dallas, Texas 75275 USA; §School of Mathematics and Statistics F07, University of Sydney, NSW 2006, Australia; and ¶Department of Cellular and Molecular Biology, Harvard University, Cambridge, Massachusetts 02138 USA

ABSTRACT We present experimental results on the bacterium *Salmonella typhimurium* which show that cells of chemotactic strains aggregate in response to gradients of amino acids, attractants that they themselves excrete. Depending on the conditions under which cells are cultured, they form periodic arrays of continuous or perforated rings, which arise sequentially within a spreading bacterial lawn. Based on these experiments, we develop a biologically realistic cell-chemotaxis model to describe the self-organization of bacteria. Numerical and analytical investigations of the model mechanism show how the two types of observed geometric patterns can be generated by the interaction of the cells with chemoattractant they produce.

INTRODUCTION

Conditions have been found under which chemotactic strains of the bacterium *Escherichia coli* aggregate to form stable macroscopic patterns of surprising complexity. These patterns form when cells, inoculated on semisolid agar, respond to gradients of chemical attractants that they themselves excrete (Budrene and Berg, 1991). We consider here patterns formed by a closely related species, *Salmonella typhimurium*, that are less complex and, thus, more amenable to mathematical analysis. Experiments with *S. typhimurium* are described, and a mathematical model is proposed to explain the observed self-organization of bacteria.

Patterns for *S. typhimurium* differ from those of *E. coli* in two important respects. First, in *E. coli* a swarm ring appears at the periphery of the growing colony, and elements of the pattern assemble in its wake. In *S. typhimurium*, under the conditions described here, the bacteria spread out in an unstructured lawn within which elements of the pattern later appear. Second, the patterns formed by *S. typhimurium* are less symmetrical; elements in adjacent perforated rings are not spatially correlated. However, both *E. coli* and *S. typhimurium* produce chemoattractant that causes cells to aggregate. Moreover, both sets of patterns are far more elaborate than those observed when chemotactic strains grow on media containing nutrients that are attractants (Adler, 1966; Nossal, 1972; Budrene, 1988; Wolfe and Berg, 1989; Agladze et al., 1993). They also differ from the well known traveling waves of aggregating cells of the slime mold *Dictyostelium discoideum* (Bonner, 1967) in that the structures formed by *E. coli* and *S. typhimurium* are temporally stable.

The spatial pattern potential of chemotaxis has been exploited in a variety of different biological contexts. Mathematical models of chemotaxis (along with reaction-diffusion and mechanochemical models) are part of the general area of integro-differential equation models for the development of spatial patterns (see Murray, 1989). Examples include pattern formation among cells of aggregating slime molds (Keller and Segel, 1970; Nanjundiah, 1973), clumps or traveling bands of bacteria (Keller and Segel, 1971; Keller and Odell, 1975; Kennedy and Aris, 1980; Lauffenburger et al., 1984), and the localization of leukocytes moving in response to bacterial inflammation (Lauffenburger and Kennedy, 1983; Alt and Lauffenburger, 1987). Most of these models for chemotactic systems have focused on aggregating *D. discoideum* cells at the stage where they do not divide, or on chemotactic bacteria whose population is assumed constant. Relatively little work has been done where cell populations are not constant. One exception is the traveling wave model of Kennedy and Aris (1980) where the bacteria reproduce and die as well as migrate. More recently, Oster and Murray (1989) proposed a cell-chemotaxis model mechanism, based on Keller and Segel (1970), for pattern generation during embryogenesis. This has been used successfully to describe pigmentation patterns in alligators (Murray et al., 1990) and in snakes (Murray and Myerscough, 1991). These studies showed that a variety of patterns can be generated from chemotaxis when significant growth occurs during the patterning process.

The outline of this paper is as follows. First, we report experimental results which show that chemotactic strains of *S. typhimurium* produce amino acids, attractants that cause cells to aggregate. When grown on succinate as a single carbon and energy source, *S. typhimurium* forms periodic arrays of continuous or perforated rings. Our goal is to explain how the cells generate these geometric patterns, rather than random aggregates. So, we develop a mathematical model based on the known biology that incorporates a nonconstant population of chemotactically driven cells that both produce and consume chemoattractant; the cells and chemoattractant both diffuse. Next we present numerical simulations which show that the model reproduces the observed complex biological patterns, and is thus a plausible mechanism for the self-organization of

Received for publication 23 May 1994 and in final form 19 January 1995.

Address reprint requests to Dr. Howard C. Berg, Department of Molecular and Cellular Biology, Harvard University, 16 Divinity Avenue, Cambridge, MA 02138-2020. Tel.: 617-495-0924; Fax: 617-495-9300; E-mail: hberg@biosun.harvard.edu.

0006-3495/95/05/2181/09 $2.00

S. typhimurium. Finally, we discuss implications of the model and its significance for future experimental and theoretical work.

EXPERIMENTAL RESULTS

Formation of geometric patterns in soft agar

Formation of geometric patterns takes place in cultures of *S. typhimurium* growing in soft agar on intermediates of the tricarboxylic acid cycle, such as succinate. Periodic structures comprised of continuous or perforated rings, corresponding to regions of high cell density, form as shown in Fig. 1. Here, the agar serves as an inert gel-like matrix that suppresses convection. At low concentrations, it is readily penetrated by motile bacteria.

The time evolution of the patterns is shown in Fig. 2. After about 24 h of growth at the region of inoculation, the bacteria start to spread radially, forming an unstructured lawn with the highest cell density at the point of inoculation. This lawn expands in radius at the rate of about 1 mm/h, as shown in Fig. 2 *A*. The cell density is higher near the center of this lawn than at its periphery. Unlike the case for *E. coli*, a traveling band does not form at the outer boundary of the lawn; nor does aggregation occur in the wake of such a band. Instead, after about 40 h of growth, pattern formation begins in the central part of the colony and spreads sequentially outwards. A structured phase propagates into a nonstructured one. Rings or perforated rings, both of which span the full thickness of the agar, form at a fixed distance from one another (about 2 mm). Once the first three rings have formed, the others appear with a fixed temporal periodicity (about 2.5 h). The spatial and the final temporal periodicities do not depend on succinate concentration. However, the time intervals for formation of the first three rings are substantially shorter than 2.5 h for growth on 5 mM succinate and longer than 2.5 h for growth on 10 mM succinate. A new ring begins at one or several points at a given radius and propagates circumferentially, both clockwise and counterclockwise. Depending upon the concentration of the substrate, the time required for the completion of a ring varies from about 70 min (5 mM succinate) to about 40 min (10 mM succinate). At lower concentrations of succinate, the ring breaks into discrete arcs or spots immediately after it forms, as shown in Fig. 2, *B* and *C*. However, the positions of spots in successive rings are not correlated. At higher concentrations, the ring remains intact but thickens somewhat until the next ring begins to form. When this happens, the cell density decreases sharply between the new ring and the previous one. Once formed, the rings (or perforated rings) remain stationary.

Microscopic observations reveal that cells are fully motile in the unstructured lawn and in newly formed rings. However, they are nonmotile in older rings. The final cell density increases with succinate concentration, but the cell doubling time remains constant over the range of concentrations that generate patterns (about 2 h for 5–15 mM succinate at 25°C). Pattern formation does not occur with strains defective for chemotaxis toward aspartate, and ring formation can be suppressed by addition of saturating amounts of chemicals that are sensed by the aspartate receptor. Therefore, chemotaxis toward aspartate or at least one of its analogs is required.

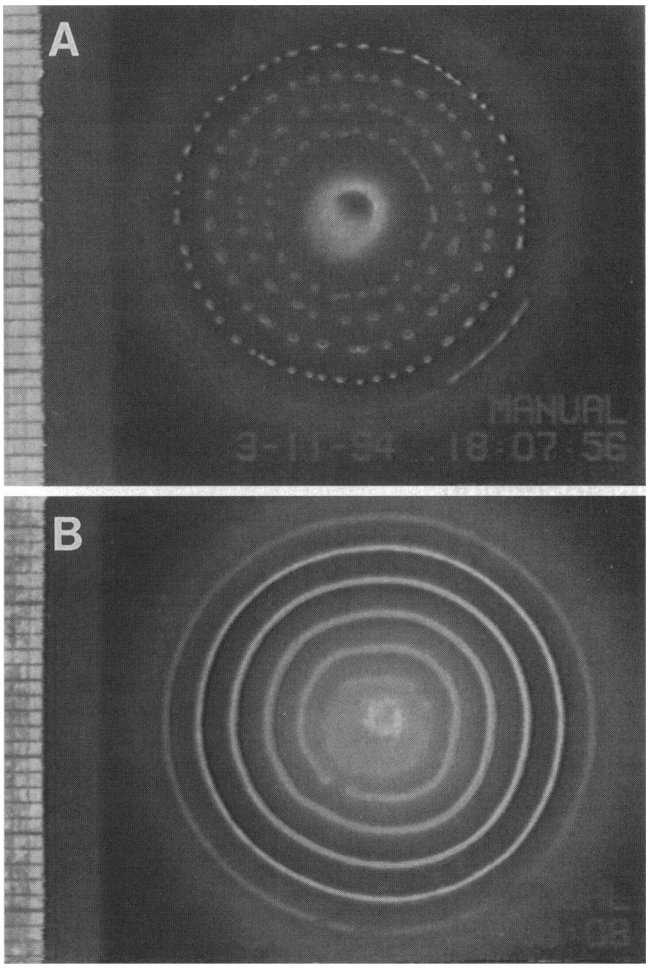

FIGURE 1 Patterns formed by *S. typhimurium* strain LT-2, visualized by scattered light: (*A*) perforated rings (spots), (*B*) rings. A 1-mm grid appears at the left edge of each picture. About 10^4 bacteria, grown on M9 glycerol medium (Miller, 1972), were inoculated at the center of an 8.5-cm-diameter petri plate containing 10 ml of soft agar (0.24%, Difco Laboratories, Inc., Detroit, MI) in M9 succinate (5 mM potassium succinate in *A*, 10 mM in *B*). The vital dye tetrazolium violet (50 μg/ml, Sigma Chemical Co., St. Louis, MO) was added to enhance image contrast. The plates were incubated at 25°C (for 48 h in *A*, 70 h in *B*). Each figure is a single frame from a time-lapse recording made with a Hamamatsu model XC-77 CCD camera on a JVC model BR-9000U cassette recorder and printed with a Sony model UP-870 MD video printer. The recording was made against a flat-black background with illumination slantwise from below (see Budrene and Berg, 1991).

Aggregation in liquid media

More can be learned about the relevant biological parameters by generating patterns in liquid media. If a suspension of *S. typhimurium* (about 10^8 cells/ml in M9 glycerol medium or in tryptone broth at 25°C) is poured into a petri plate and succinate is added (to a final concentration of 5 mM), an initially uniform suspension of bacteria transforms into a

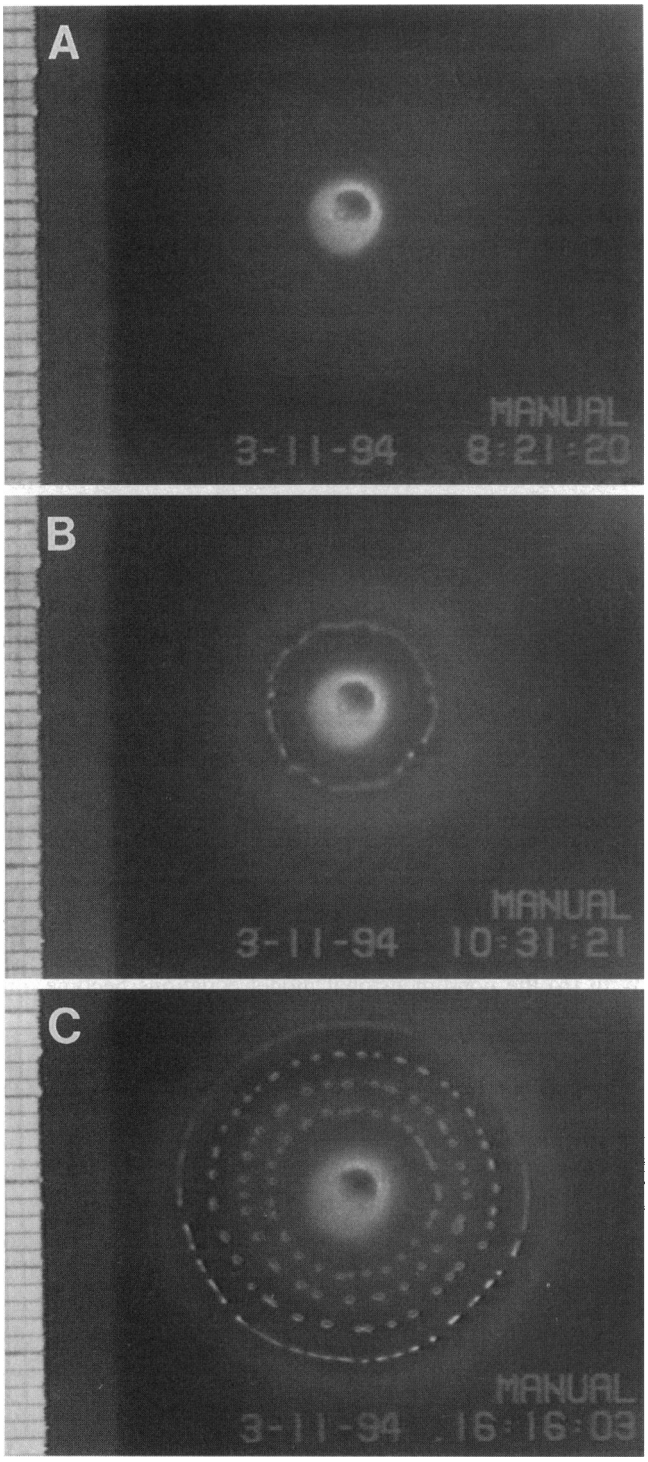

FIGURE 2 Time-evolution of the pattern shown in Fig. 1 *A*. Time after inoculation: (*A*) 38 h, (*B*) 40 h, (*C*) 46 h. A 1-mm grid appears at the left edge of each picture. Other conditions were as in Fig. 1 *A*. Note in *C* that the ring that first appeared in *B* has now broken up more completely, whereas the outermost ring is still partially intact.

field of aggregates of high cell density within 3–5 min. The distribution of these aggregates has no apparent symmetry. When fully developed, the aggregates are about 0.5 mm in diameter and are spaced irregularly over distances ranging from a fraction of a mm to 1–2 mm, depending on specific conditions. The cells in the aggregates are highly motile, and relatively few cells are found between aggregates. After about 30–45 min, the aggregates gradually disperse and the suspension becomes uniform. Amino acid analyses of supernatant fractions obtained from such experiments show that cells excrete large amounts of aspartate and glutamate. Both of these amino acids are known to bind to the same site on the aspartate receptor; however, aspartate has a much higher affinity. Therefore, it is the dominant species. After about 30–45 min, the concentration of aspartate is high enough to saturate the chemotactic response. As found with experiments in soft agar, aggregation in liquid requires a functioning aspartate receptor and can be suppressed by addition of aspartate or its analogs.

From these experiments, we conclude that patterns, albeit of low symmetry, can be formed over a time span in which changes in cell number and in concentration of substrate are small. Pattern formation requires redistribution of cell density. We believe that this occurs by the following mechanism. Addition of succinate causes the cells to excrete attractants, and fluctuations in local cell density lead to formation of gradients of these attractants. The cells, guided by chemotaxis, drift toward sites of higher cell density. As a consequence, the intervening regions are depleted of cells and, thus, of the source of attractant; therefore, initially small inhomogeneities in concentrations of cells and attractants are amplified. Presumably, the same mechanisms also play an important role for pattern formation in soft agar. It remains to be explained how, in this case, the cells form geometric patterns, rather than random aggregates.

CELL-CHEMOATTRACTANT MODEL MECHANISM

Given the detailed biological experiments described in the previous section, we hypothesize that it is the interaction between the cells and chemoattractant that causes self-organization into the observed patterns. The cells proliferate and produce chemoattractant; they only sense this chemoattractant not the substrate. In semi-solid medium, given possible long term changes in metabolic state, the cells also consume attractant. The cells and chemoattractant are both diffusive. In this section, it is our goal to give a biologically based mathematical description of the way in which these processes combine to produce regular patterns in growing cultures.

We denote the density of the (motile) cells by n, the concentration of chemoattractant by c,[1] and the concentration of the substrate by s. In the *S. typhimurium* experiments (described in Experimental Results), the consumption of substrate is negligible. Therefore, we assume that the substrate concentration is constant, thus s is just a parameter. Since there is no variation of the patterns through the thickness of the agar, the system described above can be formulated in

[1] In the model, we do not distinguish between aspartate and glutamate; instead, we consider a single attractant, sensed by the aspartate receptor.

two dimensions as:

$$\frac{\partial n}{\partial t} = \text{rate of change of cell density} \tag{1}$$

$$D_n \nabla^2 n - \nabla \cdot \left(\frac{k_1 n}{(k_2 + c)^2} \nabla c \right) + f(n,c,s)$$

diffusion; chemotaxis; proliferation

$$\frac{\partial c}{\partial t} = \text{rate of change of chemoattractant} \tag{2}$$

$$D_c \nabla^2 c + g(n,c,s) - h(n,c,s)$$

diffusion; production by cells; consumption by cells

where D_n and D_c are the diffusion coefficients of the cells and chemoattractant, respectively.

Chemotaxis drift rates are known to be proportional to the time rate of change in receptor occupancy; thus, the functional form for the chemotactic response is the one determined experimentally, with k_2 the receptor dissociation constant (Brown and Berg, 1974; Lapidus and Schiller, 1976; Weis and Koshland, 1988). For low levels of chemoattractant concentration, $c \ll k_2$, the chemotactic response of the cells is directly proportional to the gradient of c, with the parameter k_1 the constant of proportionality. As c increases, however, sensitivity to gradients of c decreases. Experimentally, steep gradients in c are not observed without large values of c.

For most substrates, the growth rate of bacteria is independent of substrate concentration, when the concentration is in the millimolar range (Neidhardt et al., 1990). The substrate, s, lies in this range during pattern generation in *S. typhimurium*. It is also known that the growth rate is independent of the chemoattractant concentration, c, and is constant with respect to cell density, n, except at extremely high cell densities when the rate of cell division drops to zero. This higher value of n is thought to be attained in the experiments. Hence, we use the following logistic form for the growth rate:

$$f(n,c,s) = k_3 n \left(1 - \frac{n}{k_4 s}\right). \tag{3}$$

The intrinsic linear growth rate is k_3, and k_4 is the carrying capacity of the substrate.

Less is known about the functional forms for the production and consumption of chemoattractant. We choose the simplest forms possible that are consistent with the experimental observations. The production of chemoattractant by the cells is zero for substrate concentration, s, below a certain threshold and constant for s above a certain threshold. In the range of the *S. typhimurium* experiments, which is between these two limits, the rate of production of chemoattractant is approximately linear in s. The production of chemoattractant is also linear in the cell density, n, until n becomes extremely large when it saturates. This suggests the following functional form for the production of the chemoattractant:

$$g(n,c,s) = \frac{k_5 s n}{k_6 + n}. \tag{4}$$

Here k_5 is the maximum production rate of chemoattractant by the cells and k_6 is the concentration of cells required for half-maximal production.

We expect consumption of chemoattractant to be governed by Michaelis-Menten kinetics. However, in the appendix we show that given (4) it is necessary to choose

$$h(n,c,s) = \frac{k_7 c n^r}{k_8 + c}, \tag{5}$$

where $r < 1$ for patterns to propagate from an initial disturbance. Here k_7 is the maximum consumption rate of the chemoattractant by the cells, and k_8 is the equivalent Michaelis (or half-saturation) constant.

It is convenient to cast the model in nondimensional terms (see Murray (1989) for a general discussion), because it reduces the number of relevant parameters by combining them into meaningful groups. So we introduce the following dimensionless quantities:

$$x^* = \frac{x}{L}, n^* = \frac{n}{k_4}, c^* = \frac{c}{C}, t^* = \frac{t}{\tau}, \tau = \frac{k_8}{k_4^r k_7}, C = \frac{\tau k_4 k_5}{k_6}, D_n^* = \frac{\tau D_n}{L^2}, D_c^* = \frac{\tau D_c}{L^2}, \alpha = \frac{\tau k_1 C}{L^2 k_2^2}, \beta = \frac{C}{k_2}, \gamma = \frac{k_4}{k_6}, \delta = \frac{C}{k_8}, \rho = \tau k_3. \tag{6}$$

Here the length scale L is yet to be determined; but note that we have $L^2/\tau = D_n/D_n^* = D_c/D_c^*$.

With (6) the nondimensional model equations become, on dropping the asterisks,

$$\frac{\partial n}{\partial t} = D_n \nabla^2 n - \alpha \nabla \cdot \left(\frac{n}{(1 + \beta c)^2} \nabla c \right) + \rho n \left(1 - \frac{n}{s}\right) \tag{7}$$

$$\frac{\partial c}{\partial t} = D_c \nabla^2 c + \frac{sn}{1 + \gamma n} - \frac{c n^r}{1 + \delta c}, \tag{8}$$

where D_n and D_c are the diffusion coefficients of the cells and chemoattractant, respectively. The parameter α measures the strength of chemotaxis, ρ the rate of proliferation, and s (assumed constant) the substrate concentration. The parameters β, γ, and δ measure the saturation of the chemoattractant sensitivity (at high levels of chemoattractant), production (at high levels of cells), and consumption(at high levels of chemoattractant).

The relative magnitudes of the model parameters determine which processes dominate the solution to these equations. With mutant cells that do not produce chemoattractant ($c = 0$) or are not sensitive to the chemoattractant ($\alpha = 0$), Eq. 7 reduces to Fisher's equation (see Murray, 1989). In this case, the cells simply spread out from the initial inoculum, and no patterns occur, as noted in Experimental Results. Normal strains produce chemoattractant to which they respond to form aggregates. It is the interplay between spreading (diffusion and proliferation) and aggregation that causes the propagating pattern, as we demonstrate in the next section.

PROPAGATING PATTERNS

In this section, in our investigation of the model mechanism (Eqs. 7 and 8), we assume for simplicity that $r = 0$ and $\delta = 0$, so that the chemoattractant is linearly degraded. Patterns are certain to form when all spatially constant solutions are unstable, since then the initial inoculum must evolve to a heterogeneous state. Equations 7–8 have one positive homogeneous steady state, $\bar{n} = s$, $\bar{c} = s^2 / (1 + \gamma s)$, in addition to the trivial steady state, $n = 0, c = 0$. The trivial steady state is always unstable. The positive homogeneous steady state, however, is only unstable when the parameters satisfy certain conditions, as shown in the appendix. In particular, increasing the chemotactic strength α tends to destabilize the constant steady state, whereas it is stabilized by increasing the diffusion coefficients D_n and D_c, the proliferation rate ρ, or the saturation parameters β and γ. As the roles of these parameters are clear, we assign them fixed values ($\alpha = 3.0$, $\beta = 2.0$, $\gamma = 0.2$, $\rho = 0.03$, $D_n = 0.1$, and $D_c = 0.3$) and examine the patterns that form at different values of substrate concentration s.

Equations 7–8 are solved numerically on a two-dimensional rectangular grid using a forward Euler scheme (see, e.g., Smith, 1985). The experimental patterns are generated from an initial inoculum at the center of the petri plate, so we choose as our initial conditions a 10×10 mesh point area at the center of the domain in which the cell density $n = 1.0$, with $n = 0$ elsewhere. Initially $c = 0$ everywhere. These conditions are then perturbed with ±1% random noise to break the symmetry. Since experimentally the cells are confined to a dish, we impose zero flux boundary conditions. However, pattern formation (in both the experiments and the simulations) takes place well before the leading edge of the perturbation reaches the domain boundary, so the boundary conditions are not really relevant; nor is the shape of the mesh, which is a square of size 301×301 grid points. The time step used in the integrations is 0.005. The reliability of this numerical method was monitored by doubling the mesh size and halving the time-step, which produced qualitatively similar results.

With the given choice of parameters, ($\alpha = 3.0$, $\beta = 2.0$, $\gamma = 0.2$, $\rho = 0.03$, $D_n = 0.1$, and $D_c = 0.3$), the constant steady state is stable when $s < s_{min} = 0.292$ (see appendix), and we find that no patterns occur for these low values of s. As s increases beyond s_{min}, the steady state becomes unstable via a supercritical bifurcation (see Murray, 1989). At these levels of s, chemoattractant is produced rapidly enough that the chemotactic response causes shallow gradients in chemoattractant to stimulate the recruitment of cells into clusters. Consequently, we observe pattern spreading sequentially outward with rings forming at a fixed distance from one another, and then breaking up into spots, as shown in Fig. 3 *A* for $s = 1.0$. At higher values of s, the chemoattractant production is strong enough to saturate the chemotactic response and the rings do not perforate, as shown in Fig. 3 *B* for $s = 2.0$. It is interesting to note that at this level of s the constant steady state has regained stability via a subcritical bifurcation (see Murray, 1989). This means that heterogeneous solutions and the constant steady-state solution coexist; however, the initial inoculum always evolves into the spreading pattern of concentric rings. At still higher values of s, the chemotactic response is completely saturated. In this case, the only stable solution is the constant steady state, and no patterns are observed.

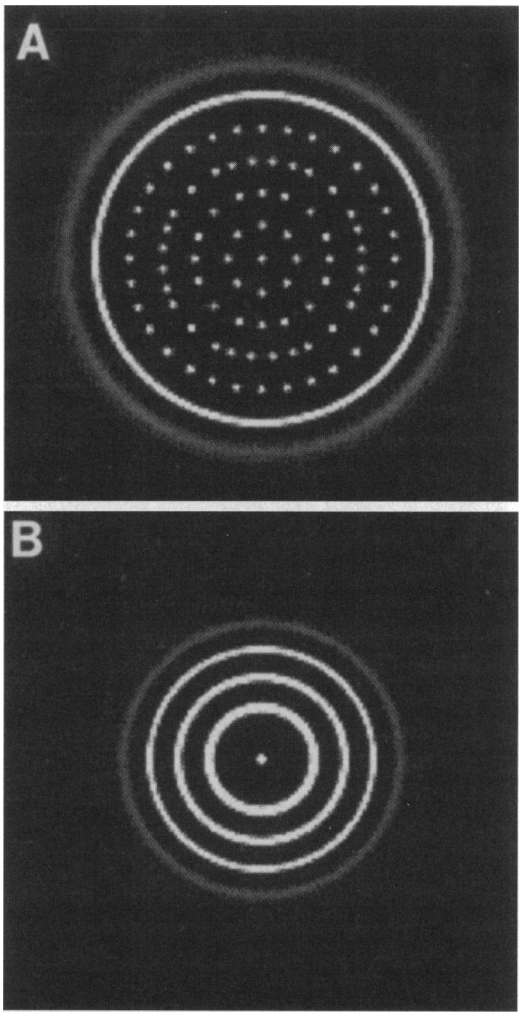

FIGURE 3 Numerical solutions of the model Eqs. 11–12 on a 3 cm×3 cm domain at time $t = 36$ h. In each case, we show only the cell density, n. The chemoattractant concentration, c, is qualitatively similar in behavior. By varying the substrate concentration, s, we can generate different patterns. For example, *A* shows perforated rings (spots) when $s = 1.0$; whereas in *B* for larger s, $s = 2.0$, we see (solid) rings. In both cases, the other parameters are $\alpha = 3.0$, $D_n = 0.1$, $D_c = 0.3$, $\rho = 0.03$, $\beta = 2.0$, and $\gamma = 0.2$.

The time evolution of the patterns is shown in Fig. 4. Here, as in Fig. 3 *A*, we choose $s = 1.0$, $\alpha = 3.0$, $\beta = 2.0$, $\gamma = 0.2$, $\rho = 0.03$, $D_n = 0.1$, and $D_c = 0.3$. By comparing the numerical simulations with the biological experiments, we estimate the length scale $L = 1.0$ mm, and the time scale $\tau = 360$ s. This gives a good correspondence with the distance between rings (20 grid points or 2 mm), and the time taken between formation of successive rings (4000 time steps or approximately 2 h). However, the initial ring evolves more quickly in the simulations than in the experiments (see Figs.

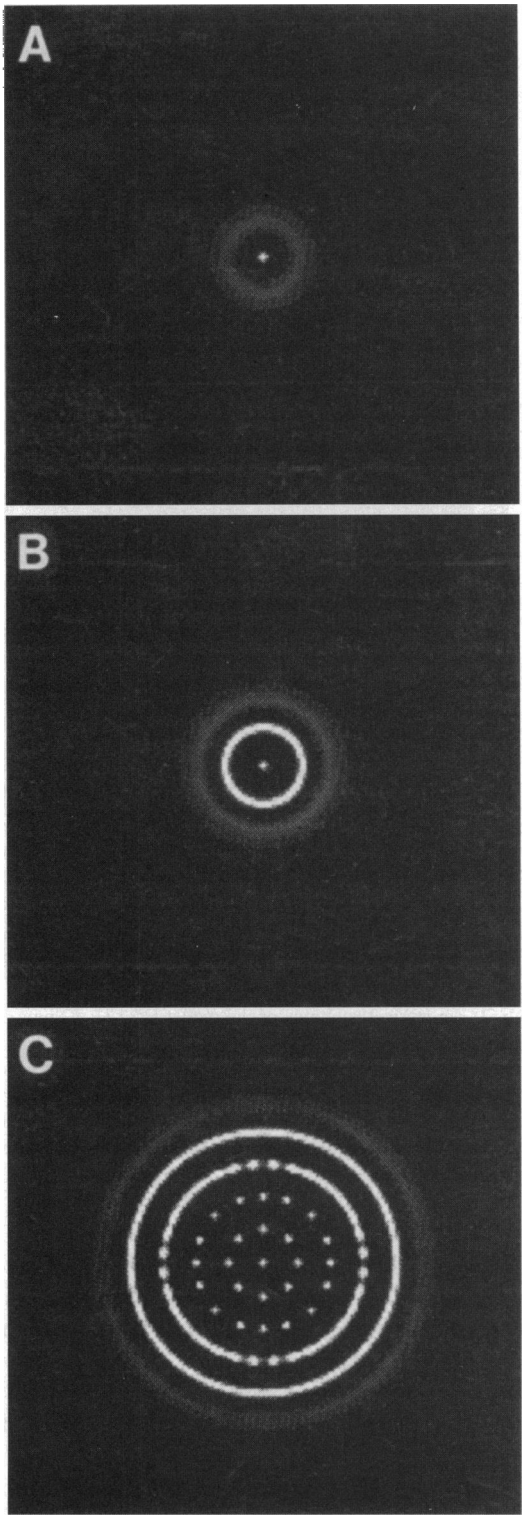

FIGURE 4 A time sequence of computed solutions of the model Eqs. 11–12: (*A*) 25 h, (*B*) 27 h, (*C*) 33 h. The domain size is 3 cm×3 cm. The parameters are as in Fig. 3 *A*.

2 *B* and 4 *B*). In the experiments, there is a substantial time lag between inoculation and formation of the bacterial lawn. The cells first grow in a compact mass and later spread out. The biological reasons for this are not known, so this stage of the process is not included in the model. Using (6), we calculate a cell diffusion coefficient of 2.8×10^{-6} cm^2/s and a chemoattractant diffusion coefficient of 8.4×10^{-6} cm^2/s. These values of the diffusion coefficients are consistent with the biological observation that D_n and D_c are the same order of magnitude, and $D_c > D_n$, with the diffusion coefficient of *S. typhimurium* depending on the manner in which cells are grown and the temperature and viscosity of the surrounding medium (Berg, 1983; Lowe et al., 1987; Berg and Turner, 1990). Furthermore, we have a cell doubling time of (ln 2)/$k_3 \approx 2.3$ h, which is also consistent with experiment (see Experimental Results).

We therefore suggest that the cell-chemoattractant mechanism (7) and (8) is a likely candidate for generating the patterns found in the *S. typhimurium* experiments. Although we assumed here, for simplicity, that the chemoattractant is linearly degraded ($r = 0$, $\delta = 0$) numerical simulations with parameter values other than those reported show that cells also self-organize into patterns when chemoattractant is consumed. For a range of substrate concentrations, the cells self-organize into rings, which are perforated at lower concentrations, but remain solid at higher concentrations, as observed experimentally. However, if the substrate concentration is too low or too high, cells spread out from the initial inoculum and no patterns are observed.

DISCUSSION

In this paper, we reported: (i) new experimental observations of complex patterns formed by chemotactic strains of *S. typhimurium*, when they aggregate in response to gradients of chemical attractant that they themselves excrete; and, (ii) based on these results, we developed a cell-chemoattractant model mechanism that enabled us to highlight, from the actual biological processes and the detailed experiments, the crucial factors involved in the self-organization of bacteria. Although we formulated our mathematical model as simply as possible, but based on the solid biological evidence for chemotaxis, we were able to verify that it is the interaction between the proliferating cells and chemoattractant they produce that is crucial to the formation of the observed geometric patterns. Response to an attractant is sufficient; repellants are not required. The similarities between the experimental patterns and the patterns from numerical solution of the model mechanism are remarkable (see Figs. 1 and 3). Moreover, estimates from the model of the cell doubling time, and of the diffusion coefficients, D_n and D_c, are consistent with experiment. Unlike in reaction-diffusion models of pattern formation, the relative role of the diffusion coefficients is not crucial mathematically. In reaction-diffusion-chemotaxis models, such as the one described here, it is the interplay between diffusion, which is stabilizing, and chemotaxis, which is destabilizing, that leads to spatially heterogeneous solutions.

The basic idea of spatial pattern formation by cells that secrete chemoattractant can easily be understood intuitively.

Fluctuations, or small perturbations, in local cell density (or alternatively in the chemoattractant concentration, or both) give rise to a greater production in chemoattractant, thereby creating local gradients in chemoattractant. The cells respond by moving up concentration gradients in chemoattractant, toward the local aggregation of cells, thus enhancing the spatial heterogeneity in the cell density. This aggregative effect, reflected in the chemotactic coefficient (α), however, is countered by the dispersal effect of random motion of the cells (D_n) and the diffusion of chemoattractant (D_c), which tend to smooth out any spatial heterogeneities. (We are not involved here with Turing structures in which diffusion is destabilizing; see, e.g., the pedagogical discussion in Murray, 1989.) The interplay between a stabilizing diffusive effect and a destabilizing chemotactic effect is crucial in the formation of spatially heterogeneous patterns. Intuitively, if the dissipative diffusion effect is too strong relative to the aggregative chemotactic effect no pattern will obtain. In the "classical" chemotaxis system (see, e.g., Oster and Murray, 1989) this gives rise to dimensionless parameters and bifurcation values for pattern to form. These bifurcation values simply give the values when the aggregative effect is balanced by the dispersal effect.

In the experiments, and the cell-chemoattractant model mechanism described in this paper, the patterning scenario is more subtle. Here the chemotactic response depends on the concentration of chemoattractant: as the concentration, c, rises, sensitivity to gradients of c decreases, and the chemoattractant response is diminished. More importantly, the substrate concentration, s, is involved in the level of production of attractant. If s is too low, the cells do not produce enough chemoattractant, on the appropriate time scale, to generate sufficiently steep gradients, and the response of the cells is too weak for the creation of local aggregations. On the other hand, if s is too high, the production of chemoattractant is so large, or so rapid, that the resulting high concentration of the attractant, c, reduces the chemotactic response and, again, the cells are not recruited into clusters. There is in fact a parameter hyperspace with bifurcation boundaries that separate pattern formation from nonpattern formation.

Unfortunately, it is not clear from these verbal descriptions that the bacteria will form anything other than random aggregates. To appreciate the fact that these processes can give rise to geometric patterns one must do a mathematical analysis. In the experiments, patterns are formed from an initial inoculum of cells at the center of the dish, with no cells elsewhere. These cells then diffuse and proliferate, and thus spread out radially. At the same time, they produce chemoattractant that causes them to aggregate. Thus, there is a growing peak of cells at the center of the dish, and a corresponding peak in chemoattractant concentration. This concentration gradient acts on the cells, inhibiting them from moving forward, and they remain in the original cluster, with the cell density highest at the point of inoculation. However, after a while, the concentration of chemoattractant, c, is sufficiently high that the chemotactic response saturates, and the cells at the leading edge of the peak move forward into a ring that is developing at the leading edge. The process then repeats itself, and a "wave of aggregation" spreads out to form regular geometric patterns. The substrate concentration, s, plays a key role in the production of chemoattractant and, thus, dictates the time for the next ring to form and the distance between rings. A procedure for determining the pattern wavelength and the speed of spread analytically is given by Myerscough and Murray (1992). The substrate concentration, s, also determines the role of local fluctuations in cell density, as described above, and hence whether the ring is solid or perforated.

By varying the amount of substrate, s, in the experiments and in the model simulations, we were able to show the spatially heterogeneous solutions include both the solid and perforated rings (compare Figs. 1 and 3). The preliminary analysis is given in the appendix, and the detailed analysis, although not trivial, we believe to be possible based on procedures already in place (Murray, 1982). There is much to be discovered from further investigation of the parameter domain of the model, using both analytical and numerical techniques. Of particular interest is the change in the model patterns from spots to rings to no pattern as chemotactic sensitivity α is decreased. This has also been experimentally observed in *E. coli* (see Budrene and Berg, 1991), where a decreasing sequence in α was achieved by adding increasing amounts of an inhibitor to the medium.

Chemotactic models are highly nonlinear, and the pattern potential is not restricted to simple elements such as stripes and regular spots (see Murray and Myerscough, 1991). However, it is not easy to predict the type of complex patterns that can be obtained because they depend intimately on the nonlinear interaction of the cells and the chemoattractant. Experimental results of Budrene and Berg (1991) showed that chemotactic strains of *E. coli* self-organize into a variety of highly regular arrays of stripes or spots. Although this paper is primarily concerned with the simple periodic patterns formed by *S. typhimurium*, there are some similarities, as well as some fundamental differences, with the complex symmetrical patterns formed by *E. coli*. A comparison of different bacterial types would be interesting, but this requires a similarly detailed modeling of *E. coli* based on the experiments. In *E. coli*, as in *S. typhimurium*, it is the interaction between proliferating cells and chemoattractant they produce that is crucial to the formation of pattern. Thus, we hypothesize that a cell-chemoattractant mechanism similar to the one described here will also be able to explain these complex patterns. However, in *E. coli*, the substrate, s, is a crucial factor in controlling pattern formation because depletion of substrate is significant: among other things, this will augment the system with another equation for the substrate concentration. Further extensive theoretical and experimental studies of patterns generated by *E. coli*, already underway, will thus be considerably more complex.

Although it is very much in its infancy — even only at the idea stage — we believe this area of pattern formation by bacterial populations could be extremely important in, for

example, detection of pollutants at low levels because in many situations small changes in the conditions of the experiments can be detected in the different patterns that are obtained. It is also a very rich field from a truly interdisciplinary viewpoint because, with the refinement of both experiments and modeling that has resulted from this study on *S. typhimurium*, we have gained insight into both the biology of bacterial pattern formation and its realistic modeling. Although there are certain gross similarities among different bacterial patterning situations, we feel that progress in understanding the basic mechanisms involved with a specific bacterial population is a prerequisite to making reliable comparisons between populations: this paper is concerned with the former.

This work was supported in part by grant DMS-9106848 (J. D. Murray) and by grant IBN-9104778 (E. O. Budrene, H. C. Berg) from the National Science Foundation. R. Tyson acknowledges a NSERC PGS-B from the Canadian Government. D. E. Woodward and M. R. Myerscough thank the Applied Mathematics Department at the University of Washington for the kind hospitality during their visits. We also thank J. Cook, T. Höfer, and P. K. Maini for help with initial formulation of the model.

MATHEMATICAL APPENDIX

Cell-chemotaxis model

We consider the following nondimensionalized system:

$$\frac{\partial n}{\partial t} = D_n \nabla^2 n - \alpha \nabla \cdot \left(\frac{n}{(1+\beta c)^2} \nabla c \right) + \rho n \left(1 - \frac{n}{s} \right) \tag{A1}$$

$$\frac{\partial c}{\partial t} = D_c \nabla^2 c + \frac{s n^p}{1+\gamma n^q} - \frac{c n^r}{1+\delta c} \tag{A2}$$

where n denotes cell density and c denotes concentration of chemoattractant. The parameter α measures the strength of chemotaxis, ρ the rate of proliferation, and s (assumed constant) the substrate concentration. Here we have introduced a more general functional form for the production and consumption of chemoattractant than that used in the text. It is worth noting, if $r = 0$ and $p = q = 1$, we have linear degradation and Michaelis-Menten production of chemoattractant by cells, whereas if $r = 1$ and $p = q = 2$, we have linear consumption and sigmoidal production. In either case, γ and δ measure the saturation in chemoattractant production and consumption (or degradation), respectively, whereas β measures the saturation in sensitivity (at high levels of chemoattractant).

Linear analysis

Equations A1–A2 have a positive steady-state solution:

$$\bar{n} = s, \bar{c} = \frac{s^{p+1}}{s^r(1+\gamma s^q) - \delta s^{p+1}}. \tag{A3}$$

For the linear stability analysis we set $n = \bar{n} + u = s + u$, and $c = \bar{c} + v$, where $|u|$ and $|v|$ are small. Substituting for n and c into (A1)–(A2) and ignoring higher order terms, we get the linear equations:

$$\frac{\partial u}{\partial t} = D_n \nabla^2 u - \left(\frac{\alpha s}{(1+\beta \bar{c})^2} \right) \nabla^2 v - \rho u \tag{A4}$$

$$\frac{\partial v}{\partial t} = D_c \nabla^2 v + \frac{s^p}{1+\gamma s^q} \left(p - \frac{\gamma q s^q}{1+\gamma s^q} - r \right) u - \frac{s^r}{(1+\delta \bar{c})^2} v \tag{A5}$$

We now look for solutions of the form $(u,v) \alpha \exp[i\mathbf{k}\cdot\mathbf{x} + \lambda t]$, where $\mathbf{k}$ is the wave number, which measures the size of the patterns, and λ is the dimensionless growth rate. The growth rate $\lambda(k^2)$ is the appropriate solution of the dispersion relation

$$\lambda^2 + \lambda \left(k^2(D_n + D_c) + \rho + \frac{s^r}{(1+\delta \bar{c})^2} \right) + D_n D_c k^4 + M k^2 + \frac{\rho s^r}{(1+\delta \bar{c})^2} = 0 \tag{A6}$$

where

$$M \equiv \frac{D_n s^r}{(1+\delta \bar{c})^2} + \rho D_c - \left(\frac{\alpha s^{p+1}}{(1+\beta \bar{c})^2 (1+\gamma s^q)} \right) \left(p - \frac{\gamma q s^q}{1+\gamma s^q} - r \right). \tag{A7}$$

Because the experimental patterns only occur when the bacteria are both motile and chemotactic, we require the positive steady-state $(\bar{n},\bar{c})$ to be stable in the absence of spatial effects ($D_n = 0, \alpha = 0$). This is easily verified: $\mathrm{Re}(\lambda(k^2 = 0)) < 0$. The homogeneous solution is unstable to spatial disturbances if $\mathrm{Re}(\lambda(k^2)) > 0$ for some wave number $\mathbf{k} \neq \mathbf{0}$. When $\lambda = 0$, k^2 satisfies

$$D_n D_c k^4 + M k^2 + \frac{\rho s^r}{(1+\delta \bar{c})^2} = 0. \tag{A8}$$

For unstable modes to exist we require that at least one root of (A8) is real and non-negative, namely,

$$M < 0, \tag{A9}$$

and

$$M^2 > \frac{4 \rho s^r D_n D_c}{(1+\delta \bar{c})^2}. \tag{A10}$$

In particular, from (A7) and (A9), for heterogeneous solutions, we require $\alpha > 0$, and

$$p - \frac{\gamma q s^q}{1+\gamma s^q} - r > 0. \tag{A11}$$

First, note that we are not involved here with Turing structures in which diffusion is destabilizing: (A9) cannot be satisfied by increasing D_n, or D_c. Furthermore, as remarked in the text, if the production of the chemoattractant by the cells is assumed to be a Michaelis-Menten function ($p = q = 1$) then we must have $r < 1$, that is, the cells cannot linearly consume the chemoattractant.

We choose to investigate the simplest case, namely, $p = 1$, $q = 1$, $r = 0$, and $\delta = 0$. Then from (A9) and (A10), we have the condition for heterogeneous solutions:

$$A\beta s^2 + (A\gamma - \sqrt{\alpha})\, s + A < 0, \tag{A12}$$

where

$$A^2 = D_n + \rho D_c + 2\sqrt{\rho D_n D_c}.$$

From this we see that increasing α has a destabilizing effect, whereas increasing β, γ, ρ, D_n, or D_c has a stabilizing effect. The role of s when it is a parameter is less clear: it can be both stabilizing and destabilizing. With the given choice of parameters, ($\alpha = 3.0$, $\beta = 2.0$, $\gamma = 0.2$, $\rho = 0.03$, $D_n = 0.1$, and $D_c = 0.3$), the constant steady state is unstable for $0.292 < s < 1.715$.

REFERENCES

Adler, J. 1966. Chemotaxis in bacteria. *Science.* 153:708–716.

Agladze, K., L. Budriene, G. Ivanitsky, V. Krinsky, V. Shakhbazyan, and M. Tsyganov. 1993. Wave mechanisms of pattern formation in microbial populations. *Proc. R. Soc. Lond. B. Biol. Sci.* 253:131–135.

Alt, W., and D. A. Lauffenburger. 1987. Transient behaviour of a chemotaxis system modelling certain types of tissue inflammation. *J. Math. Biol.* 24:691–722.

Berg, H. C. 1983. Random Walks in Biology. Princeton University Press, Princeton, NJ. 190 pp.

Berg, H. C., and L. Turner. 1990. Chemotaxis of bacteria in glass capillary arrays. *Biophys. J.* 58:919–930.

Bonner, J. T. 1967. The Cellular Slime Molds, 2nd Ed. Princeton University Press, Princeton, NJ. 205 pp.

Brown, D. A., and H. C. Berg. 1974. Temporal stimulation of chemotaxis in *Escherichia coli*. *Proc. Natl. Acad. Sci. USA.* 71:1388–1392.

Budrene, E. O. 1988. Effect of chemotaxis on geometry of the structures in bacterial colonies. *Biophysika.* 33:373–375.

Budrene, E. O., and H. C. Berg. 1991. Complex patterns formed by motile cells of *Escherichia coli*. *Nature.* 349:630–633.

Keller, E. F., and G. M. Odell. 1975. Necessary and sufficient conditions for chemotactic bands. *Math. Biosci.* 270:309–317.

Keller, E. F., and L. A. Segel. 1970. Initiation of slime mold aggregation viewed as an instability. *J. Theor. Biol.* 26:399–415.

Keller, E. F., and L. A. Segel. 1971. Travelling bands of chemotactic bacteria: a theoretical analysis. *J. Theor. Biol.* 30:235–248.

Kennedy, C. R., and R. Aris. 1980. Travelling waves in a simple population model involving growth and death. *Bull. Math. Biol.* 42:397–426.

Lapidus, I. R., and R. Schiller. 1976. Model for chemotactic response of a bacterial population. *Biophys. J.* 16:779–789.

Lauffenburger, D. A., M. Grady, and K. H. Keller. 1984. An hypothesis for approaching swarms of myxobacteria. *J. Theor. Biol.* 110:257–274.

Lauffenburger, D. A., and C. R. Kennedy. 1983. Localised bacterial infection in a distributed model for tissue inflammation. *J. Math. Biol.* 16:141–163.

Lowe, G., M. Meister, and H. C. Berg. 1987. Rapid rotation of flagellar bundles in swimming bacteria. *Nature.* 325:637–640.

Miller, J. H. 1972. Experiments in Molecular Genetics. Cold Spring Harbor Laboratory Press, Cold Spring Harbor, NY. 466 pp.

Murray, J. D. 1982. Parameter space for Turing instability in reaction diffusion mechanisms: a comparison of models. *J. Theor. Biol.* 98:143–163.

Murray, J. D. 1989. Mathematical Biology. Springer-Verlag, Berlin. [2nd corrected edition 1993]. 760 pp.

Murray, J. D., D. C. Deeming, and M. W. J. Ferguson. 1990. Size-dependent pigmentation-pattern formation in embryos of *Alligator mississippiensis*: time of initiation of pattern generation mechanism. *Proc. R. Soc. Lond. B. Biol. Sci.* 239:279–293.

Murray, J. D., and M. R. Myerscough. 1991. Pigmentation pattern formation on snakes. *J. Theor. Biol.* 149:339–360.

Myerscough, M. R., and J. D. Murray. 1992. Analysis of a propagating pattern in a chemotaxis system. *Bull. Math. Biol.* 54:77–94.

Nanjundiah, V. 1973. Chemotaxis, signal relaying and aggregation morphology. *J. Theor. Biol.* 42:63–105.

Neidhardt, F. C., J. L. Ingraham, and M. Schaechter. 1990. Physiology of the Bacterial Cell. Sinauer Associates, Inc., Sunderland, MA. 506 pp.

Nossal, R. 1972. Growth and movement of rings of chemotactic bacteria. *Exp. Cell Res.* 75:138–142.

Oster, G. F., and J. D. Murray. 1989. Pattern formation models and developmental constraints. *J. Exp. Zool.* 251:186–202.

Smith, G. D. 1985. Numerical Solutions of Partial Differential Equations: Finite Difference Methods. Oxford University Press, Oxford. 337 pp.

Weis, R. M., and D. E. Koshland, Jr. 1988. Reversible receptor methylation is essential for normal chemotaxis of *E. coli* in gradients of aspartic acid. *Proc. Natl. Acad. Sci. USA.* 85:83–87.

Wolfe, A. J., and H. C. Berg. 1989. Migration of bacteria in semi-solid agar. *Proc. Natl. Acad. Sci. USA.* 86:6973–6977.